Biochemical Pharmacology, Vol. 39, No. 9, pp. 1411–1421, 1990.
Printed in Great Britain.

0006-2952/90 $3.00 + 0.00

THE FATE OF *N*1′-METHANESULPHONYL-*N*4′-(9-ACRIDINYL)-3′-METHOXY-2′,5′-CYCLOHEXADIENE-1′,4′-DIIMINE (*m*-AQDI), THE PRIMARY OXIDATIVE METABOLITE OF AMSACRINE, IN TRANSFORMED CHINESE HAMSTER FIBROBLASTS*

MAXINE A. ROBBIE, BRIAN D. PALMER,† WILLIAM A. DENNY† and WILLIAM R. WILSON‡

Section of Oncology, Department of Pathology and † Cancer Research Laboratory, University of Auckland School of Medicine, Private Bag, Auckland, New Zealand

(*Received* 13 *September* 1989; *accepted* 21 *November* 1989)

Abstract—The cytotoxicity of the anti-leukaemia drug amsacrine (*m*-AMSA) has been suggested to result from its oxidative metabolism to the corresponding quinonediimine, *N*1′-methanesulphonyl-*N*4′-(9-acridinyl)-3′-methoxy-2′,5′-cyclohexadiene-1′,4′-diimine (*m*AQDI). The metabolic fate of *m*AQDI was examined in cultured CHO cells (subline AA8) to identify the end products to be expected following oxidative metabolism of *m*-AMSA. [*Acridinyl-G*-^{3}H]-*m*-AQDI was rapidly accumulated by AA8 cells in phosphate buffered saline with complete conversion in less than one minute to *m*-AMSA, macromolecular adducts and polar low molecular weight species, each of these three classes being formed in approximately equal amounts. Two of the polar products were chromatographically identical to those formed on reaction of *m*-AQDI with reduced glutathione. These were identified by ^{1}H NMR spectroscopy as the 1,4-addition product 5′-(*S*-glutathionyl)-*m*-AMSA and the previously unreported isomeric 6′-(*S*-glutathionyl)-*m*-AMSA. These thiol adducts were also formed rapidly from *m*-AQDI in deproteinized cell lysates indicating a non-enzymatic process, although the possibility of enzymatic catalysis in intact cells has not been eliminated. The absence of such products in AA8 cells after treatment with *m*-AMSA places an upper limit of 1% per hour on the rate of its oxidative metabolism in these cells and suggests that generation of *m*-AQDI is unlikely to be responsible for the cytotoxicity of *m*-AMSA in cultured tumour cells.

Amsacrine (4′-[9-acridinylamino]methanesulphon-*m*-anisidide; *m*-AMSA§) is a synthetic DNA intercalating agent with useful clinical activity against acute leukaemias [1]. Like many other DNA intercalating agents, *m*-AMSA is able to induce DNA lesions by stabilizing the formation of a "cleavable complex" between DNA topoisomerase II (EC 5.99.1.3) and DNA [2, 3]. There is a correlation between the production of the topoisomerase II complex and cell killing by *m*-AMSA and related anilinoacridine antitumour agents [4]. However, the relationship between these readily reversible DNA lesions and the more long-lived chromosome breaks that appear to be responsible for cell killing by intercalating antitumour drugs [5, 6] remains poorly understood.

An alternative hypothesis for the mode of action of *m*-AMSA proposes bioactivation to a reactive metabolite [7–9]. *m*-AMSA is extensively metabolized in blood [10, 11] and in the liver [12] via two major routes, both of which result in formation of conjugates with thiols. The first involves nucleophilic attack of the sulphydryl group at the C-9 position of the acridine ring resulting in formation of the 9-acridinyl thioether [10, 13, 14]. The second occurs via cytochrome P-450-dependent oxidation to the corresponding quinone diimine, *N*1′-methanesulphonyl-*N*4′-(9-acridinyl)-3′-methoxy-2′,5′-cyclohexadiene-1′,4′-diimine, *m*-AQDI, which is highly reactive toward conjugate addition of GSH or other nucleophiles to the diimine ring [7, 15, 16].

Both *m*-AQDI and its hydrolysis product *m*-AQI are potent cytotoxic agents *in vitro* [7] and have been suggested to be responsible for the cytotoxicity of *m*-AMSA [7, 8]. The formation of similar quinoneimine

* This work was supported by grants from the Medical Research Council of New Zealand, and the Auckland Division of the Cancer Society of New Zealand.

‡ To whom correspondence should be addressed.

§ Abbreviations: *m*-AMSA, 4′-(9-acridinylamino)-methanesulphon-*m*-anisidide; *m*-AQDI, *N*1′-methanesulphonyl-*N*4′-(9-acridinyl)-3′-methoxy-2′,5′-cyclohexadiene-1′,4′-diimine; *m*-AQI, 3′-methoxy-4′-(9-acridinylamino)-2′,5′-cyclohexadien-1′-one; 5′-GS-*m*-AMSA, 4′-(9-acridinylamino)-5′-(*S*-glutathionyl)-3′-methoxymethane-sulphonanilide; 6′-GS-*m*-AMSA, 4-(9-acridinylamino)-6′-(*S*-glutathionyl)-3′-methoxymethanesulphonanilide; 6′-GS-AAMP, 4′-(9-acridinyl-amino)-6′-(*S*-glutathionyl)-3′-methoxyphenol; 9-AA, 9-aminoacridine; 9-AO, 9(10H)-acridone; AAMP, 4′-(9-acridinylamino)-3′-methoxyphenol; HPLC, high performance liquid chromatography; α-MEM, Alpha minimal essential medium; MSA, 4-amino-3-methoxymethanesulphonanilide; MeCN, acetonitrile; TEAP, triethylammonium phosphate; [^{3}H]-*m*-AMSA, [*acridinyl-G*-^{3}H]-*m*-AMSA; [^{3}H]-*m*-AQDI, [*acridinyl-G*-^{3}H]-*m*-AQDI; PBS, phosphate-buffered saline; GSH, reduced glutathione.

intermediates in the metabolism of paracetamol [17] and N^2-methyl-9-hydroxyellipticine [18] appears to play an important role in the cytotoxicity of these drugs by a mechanism involving arylation of cellular thiols. The quinoneimine derivatives of *m*-AMSA might exert their toxicity by a similar mechanism. Alternatively, since rapid cleavage of DNA has been observed in the presence of *m*-AMSA, oxygen and copper salts, a mechanism of cytotoxicity based on the production of oxygen free radicals generated by redox cycling of DNA-intercalated *m*-AQDI has been proposed [8]. However, it is not known whether these oxidative metabolites are formed *in situ* by tumour cells. The high reactivity of the quinoeimines and quinoediimines of the 9-anilinoacridines to reduction and nucleophilic attack [16] would seem to require generation in the target cell, or at least in the target tissue, particularly since the extravascular diffusion of the anilinoacridines in tissue is slow (W. R. Wilson, unpublished observations).

A previous study of *m*-AMSA metabolism in tumour cell cultures failed to demonstrate *m*-AQDI formation [19]. However, since any *m*-AQDI formed is likely to undergo rapid further metabolism this result does not necessarily preclude a role for oxidative metabolism in the cytotoxicity of *m*-AMSA. In the present study we investigate the fate of *m*-AQDI in these same tumour cells in order to assess its role in cell killing by *m*-AMSA.

MATERIALS AND METHODS

Cells. AA8 cells were maintained as subconfluent monolayers without antibiotics as previously described [20] and were used to establish suspension cultures in glass spinner flasks. The growth medium was Alpha minimal essential medium (*α*-MEM) containing 10% heat-inactivated foetal calf serum, 100 μg/mL streptomycin sulphate, and 100 I.U./mL penicillin G. Flasks were gassed with 5% CO_2 in air and incubated at 37° in a waterbath with magnetic stirring.

Chemicals. *m*-AMSA was provided as the isethionate salt by Warner-Lambert Laboratories (Ann Arbor, MI). 9-Aminoacridine (9-AA) was purchased as the hydrochloride salt from the Sigma Chemical Co. (St Louis, MO). 4-Amino-3-methoxymethanesulphonanilide (MSA) was purchased from Starks Associates Inc. (Buffalo, NY). All other compounds were synthesized in this laboratory. *m*-AQDI, *m*-AQI and 9(10H)-acridone (9-AO) were all used as the free bases. The reduction product of *m*-AQI(4′-[9-acridinylamino]-3′-methoxyphenol; AAMP) was used as the hydrochloride salt. Purities were tested using a Waters Associates (Milford, MA) HPLC system equipped with a reverse-phase Novapak C_{18} Radial-PAK column. Unless otherwise indicated the mobile phase was 18% (v/v) acetonitrile (MeCN) in 10 mM triethylammonium phosphate (TEAP), pH 3.0, at a flow rate of 2.5 mL/min. The eluate was analysed at 254 and 436 nm with a Model 440 absorbance detector using a Waters 840 Data and Chromatography Control Station. *m*-AMSA, *m*-AQI, and 9-AO were chromatographically homogeneous while *m*-AQDI contained a trace of *m*-AQI.

Authentic samples of the GSH conjugates of *m*-AQDI and *m*-AQI were synthesized according to the method of Shoemaker *et al.* [12]. The reaction of *m*-AQI with GSH gave a single product. Under the same conditions *m*-AQDI gave two major products which were separated by HPLC using a mobile phase of 15% MeCN in 10 mM TEAP, pH 3.0. Peak fractions from 50 HPLC runs (each with 50 μg of reaction product in 0.5 mL mobile phase) were pooled, loaded onto Sep-Pak C_{18} cartridges (Waters Associates) and washed with water to remove inorganics. The products were eluted with approximately 1 mL methanol and evaporated to dryness for characterization as described below.

Radiochemicals. [*Acridinyl-G*-^{3}H-*m*-AMSA] ([^{3}H]-*m*-AMSA; 23.9 GBq/mmol) was synthesized from [*G*-^{3}H]*N*-(phenyl)anthranilic acid [10] which was prepared by catalytic exchange against ^3H_2O at the Radiochemical Centre, Amersham, U.K. The hydrochloride salt was stored as a 5 mM solution in 50% ethanol at −20°. The radiochemical purity, determined by liquid scintillation counting of the HPLC eluate, was >94%. [*Acridinyl-G*-^{3}H]-*m*-AQDI ([^{3}H]-*m*-AQDI; 24.3 GBq/mmol (was synthesized from [^{3}H]-*m*-AMSA by addition of active MnO_2 (50 μmol) to the free base of [^{3}H]-*m*-AMSA (25 μmol) in dry ethyl acetate (10 mL). The mixture was stirred for 30 min at 25° and added directly to the top of a column of silica gel 60 (200 mg; E. Merck Ltd, Darmstadt, F.R.G.) packed in ethyl acetate in a Pasteur pipette. Ethyl acetate eluted a black band which on evaporation of the appropriate fractions gave a black solid. Trituration with diethyl ether gave a crystalline material which was collected by filtration (9 mg, 90%), m.p. 217–222°. The solid was pure by TLC in two different solvent systems. Radiochemical purity could not be assessed accurately by HPLC because of reduction to *m*-AMSA during chromatography (*vide infra*). However, the extent of contamination with *m*-AMSA was similar (approximately 17%) following injection of crude [^{3}H]-*m*-AQDI or on immediate re-chromatography of an equivalent amount of the HPLC-purified species suggesting the original radiochemical purity to be at least 95%.

Metabolism studies. Suspension cultures of AA8 cells were grown to densities of 1.4×10^6 cells/mL and concentrated to 10^7 cells/mL after washing in PBS (0.17 M NaCl, 3.4 mM KCl, 10.0 mM KH_2PO_4, 18.0 mM Na_2HPO_4, 1.0 mM $CaCl_2$, 0.5 mM $MgCl_2$). The cell suspensions in PBS were equilibrated at 37° for 15 min in 25-mL spinner flasks. Drug exposures were initiated by adding [^{3}H]-*m*-AQDI to 10 μM. At varying times samples (1 mL) were centrifuged (15,000 *g*, 1 min) at room temperature, chilled on ice and supernatants were sampled for scintillation counting. The cell pellets were lysed by addition of 40 μL ice-cold water or 20 μL water followed by 25 μL of freshly-prepared spike solution (10 μM 6′-GS-AAMP, 9 μM 5′-GS-*m*-AMSA, 11 μM 6′-GS-*m*-AMSA, 5 μM-AQI, 12 μM 9-AO, 20 μM-AQDI, and 30 μM-AMSA in 18% MeCN, 10 mM TEAP, pH 3.0). Cell lysates were deproteinized by adding MeCN (450 μL, final concentration approximately 90% v/v) and centrifuging (15,000 *g*, 1 min) after 10 min at 0°. MeCN-soluble fractions were stored at −20°.

Radioactivity in the MeCN-insoluble material was determined by scintillation counting after washing the pellets three times with 90% MeCN at 0°. In each wash step the MeCN-insoluble material was resuspended in 10 μL water before adding 900 μL MeCN and centrifuging. Pooled supernatants were concentrated by evaporation before scintillation counting. Pellets were digested with 1.0 mL Protosol (New England Nuclear, Boston, MA) at 55° for 1 hr before determining radioactivity. MeCN-soluble fractions were prepared for HPLC by evaporating under a stream of oxygen-free nitrogen and dissolving the residue in 160 μL of mobile phase. Metabolites were detected by collecting fractions of the HPLC eluate for liquid scintillation counting.

Spectroscopy. The GSH adducts of *m*-AQI and *m*-AQDI were dissolved in d_6-DMSO for NMR analysis, with tetramethylsilane as an internal standard. Fourier transform ^{1}H-NMR spectra were acquired on a Bruker AM400 spectrometer at a temperature of 294°K. Spectra of each of the GSH adducts of *m*-AQDI were acquired using a 5-mm selective ^{1}H probe and that of the GSH adduct of *m*-AQI with a 5-mm dual ^{1}H-^{13}C probe. UV-visible absorbance spectra were acquired with a Pye Unicam SP8-100 spectrophotometer.

RESULTS

Characterization of the synthetic products formed by reaction of m-*AQI and* m-*AQDI with GSH*

The product from reaction of GSH with *m*-AQI was homogeneous by HPLC, eluting as a single peak with a retention time of 5.4 min. The NMR spectrum of this species (Fig. 1) enabled its identification as 4′-(9-acridinylamino)-6′-(*S*-glutathionyl)-3′-methoxyphenol (6′-GS-AAMP) on the basis of the two singlet signals from phenyl aromatic protons at δ 6.75 and 6.64 ppm, indicating their location at *para* positions on the anilino ring.

NMR: δ 8.58 (broad s, 1H, glycyl COOH), 8.46 (d, 1H, J = 7.9 Hz, glutamyl COOH), 7.91 (m, 2H, acridine aromatic), 7.48 (dd, 2H, J = 7.1 Hz, acridine aromatic), 6.75 (*s*, 1H, phenyl aromatic $H_{2'}$), 6.64 (s, 1H, phenyl aromatic $H_{5'}$), 4.32 (dd, 1H, J = 8.6, 12.9 Hz, cysteinyl α-hydrogen), 3.64 (AB quartet, 2H, glycyl methylene), 3.50 (s, 3H, OCH_3), 3.34 (t, J = 6.5 Hz, glutamyl α-hydrogen), 3.11 (dd, J = 3.8, 12.0 Hz, cysteinyl methylene), 2.89 (dd, J = 9.5, 12.9 Hz, cysteinyl methylene), 2.32 (AB quartet, 2H, J = 14.2 Hz, glutamyl γ-methylene), 1.90 (d x t, 2H, glutamyl β-methylene).

HPLC analysis indicated that the product formed

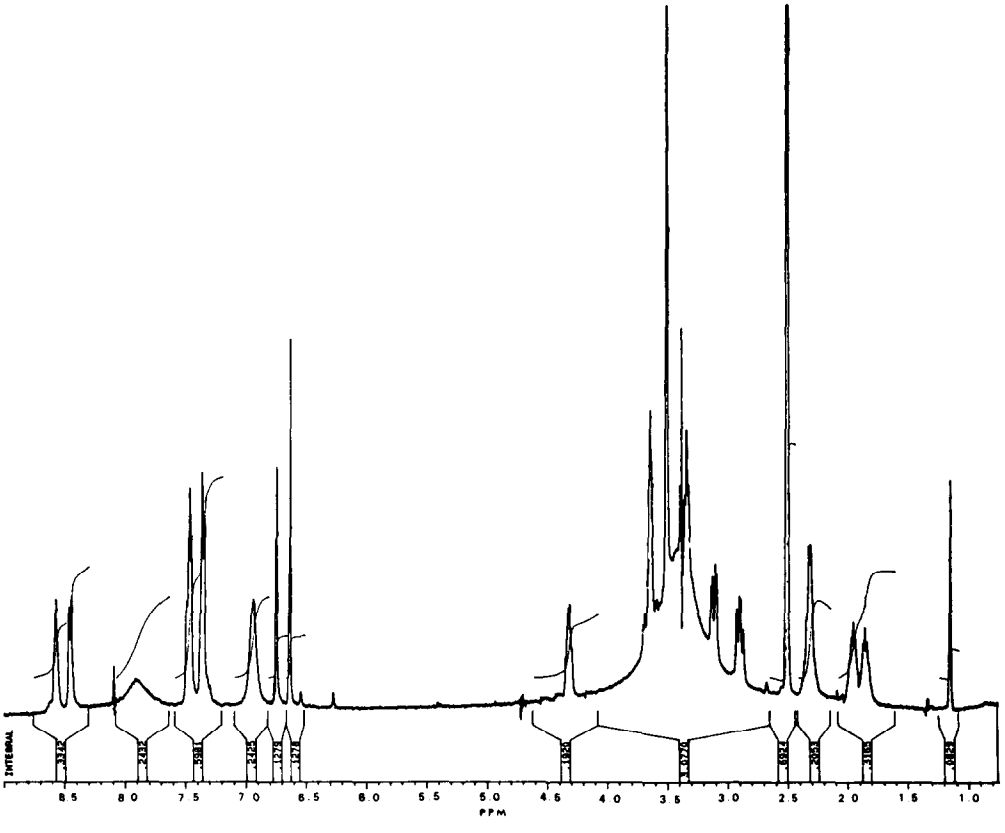

Fig. 1. ^{1}H-NMR spectrum of the glutathionyl adduct of *m*-AQI at 400 MHz. The signal at 2.51 ppm is due to DMSO.

by reacting *m*-AQDI with GSH was a mixture of two components with approximately equal peak areas. These were incompletely resolved, with retention times of 6.6 (species I) and 7.4 min (species II). Baseline resolution was achieved by reducing the MeCN content of the mobile phase from 18 to 15% giving retention times of approximately 14.6 (species I) and 17.0 min (species II). The components were purified by HPLC for NMR analysis.

NMR (species I): δ 8.45 (m, acridine aromatic, 7.84 (m, 2H, acridine aromatic), 7.33 (d, 2H, J = 8.7 Hz, acridine aromatic), 6.91 (d, 1H, J = 1.75 Hz, phenyl aromatic $H_{2'}$), 6.74 (d, 1H, J = 1.75 Hz, phenyl aromatic $H_{6'}$), 4.38 (m, cysteinyl α-hydrogen), 4.0 (2d, glycyl methylene), 3.61 (broad s, 3H, OCH_3), 3.30 (t, 1H, J = 6.5 Hz, glutamyl α-hydrogen), 3.02 (s, 3H, SO_2CH_3), 2.35-2.13 (m, glutamyl γ-methylene), 1.95–1.75 (m, glutamyl β-methylene).

NMR (species II): δ 8.62 (broad s, glycyl COOH), 8.55 (d, glutamyl COOH), 7.50 (m, acridine aromatic), 7.35 (d, acridine aromatic), 6.99 (s, 1H, phenyl aromatic, $H_{2'}$), 6.91 (s, 1H, phenyl aromatic, $H_{5'}$), 4.5 (broad, NH), 4.32 (dd, 1H, J = 5.3, 9.4 Hz, cysteinyl α-hydrogen), 3.53 (broad s, 3H, OCH_3), 3.33 (t, glutamyl α-hydrogen), 2.94 (broad s, 3H, SO_2CH_3), 2.70 (dd, cysteinyl methylene), 2.33 (m, glutamyl γ-methylene), 1.92 (m, glutamyl β-methylene).

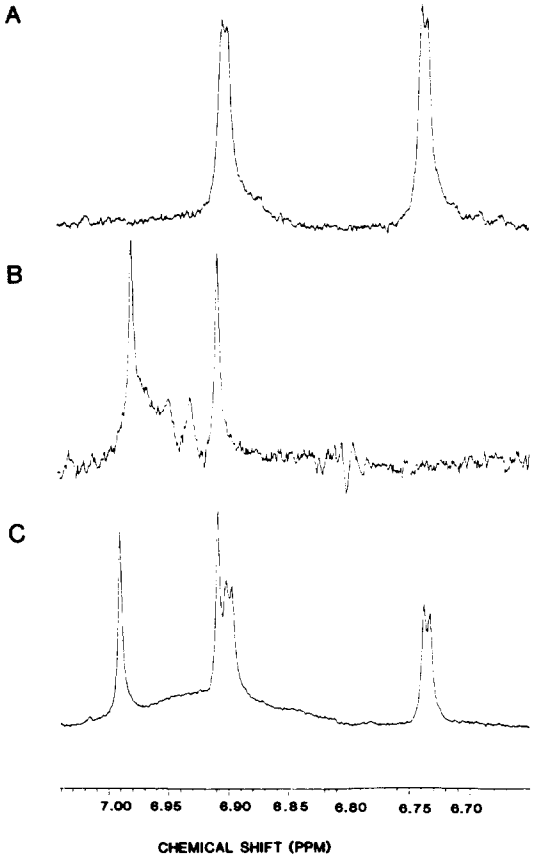

Fig. 2. ^{1}H-NMR spectra of species formed by reaction of GSH with *m*-AQDI. Regions showing the phenyl aromatic protons. (A) Species I (5′-GS-*m*-AMSA). (B) Species II (6′-GS-*m*-AMSA). (C) Unresolved mixture.

Species I was identified as the 5′-glutathionyl adduct of *m*-AMSA, 4′-(9-acridinylamino)-5′-(*S*-glutathionyl) - 3′ - methoxymethane-sulphonanilide (5′-GS-*m*-AMSA) on the basis of the two doublets at δ 6.91 and 6.74 ppm in the NMR spectrum (Fig. 2A). The coupling constant of approximately 1.75 Hz is consistent with *meta*- coupling between protons at the 2′- and 6′-positions of the anilino ring. Species II was identified as the 6′-addition product, 4′-(9-acridinylamino)-6′-(*S*-glutathionyl)-3′-methoxymethanesulphonanilide (6′-GS-*m*-AMSA), the two singlets at δ 6.99 and 6.91 ppm (Fig. 2B) indicating that absence of *ortho*- or *meta*-coupling between the remaining phenyl aromatic protons. The NMR spectrum of the unseparated synthetic mixture (Fig. 2C) showed this to be comprised of approximately equal amounts of species I (46%) and II (54%).

The UV-visible absorbance spectra of purified 5′-GS-*m*-AMSA and 6′-GS-*m*-AMSA were compared using methanol as solvent. 5′-GS-*m*-AMSA showed peaks at 207 and 224 nm, with a shoulder at 250 nm and a broad peak at 490 nm. The spectrum for 6′-GS-*m*-AMSA showed peaks at 220, 249 and 264 nm and a broad peak at 413 nm (data not shown).

The HPLC assay

The chromatographic characteristics of various potential *m*-AQDI metabolites, using the standard HPLC conditions, are described in Table 1. A representative chromatographic profile is shown in Fig. 3. 6′-GS-AAMP was the least stable of these species, while *m*-AQDI showed moderate stability with slow hydrolysis to *m*-AQI at approximately 0.5% hr^{-1} in mobile phase at 0°. Quantitation of *m*-AQDI was complicated by reduction to *m*-AMSA during chromatography as demonstrated in Fig. 4. HPLC of a 0.4 nmol sample of [^{3}H]-*m*-AQDI indicated significant contamination by [^{3}H]-*m*-AMSA. However, when a sample of [^{3}H]-*m*-AQDI was purified by HPLC and 0.1 nmol was immediately rechromatographed the ratio of *m*-AMSA to *m*-AQDI increased further. Reduction of *m*-AQDI to *m*-AMSA was most pronounced with low chro-

Table 1. HPLC characteristics of *m*-AMSA and potential metabolites on a reverse-phase C_{18} Novapak column, using a mobile phase of 18% MeCN containing 10 mM TEAP, pH 3.0, at a flow rate of 2.5 mL/min with absorbance detection at wavelengths of 254 and 436 nm

Metabolite	Retention time (min)	Peak height ratio (Abs_{254}/Abc_{436})
MSA	1.6 ± 0.1	*
9-AA	3.7 ± 0.1	98.6 ± 8.4
6′-GS-AAMP	5.4 ± 0.1	3.3 ± 0.5
5′-GS-*m*-AMSA	6.6 ± 0.2	3.4 ± 0.1
6′-GS-*m*-AMSA	7.4 ± 0.3	3.2 ± 0.1
m-AQI	11.1 ± 0.2	14.9 ± 0.5
9-AO	19.6 ± 0.5	*
m-AQDI	23.1 ± 0.4	7.2 ± 0.9
AAMP	23.7 ± 1.4	2.9 ± 0.1
m-AMSA	26.9 ± 0.7	2.7 ± 0.1

* No absorbance at 436 nm.

Errors are the standard deviations from at least six analyses.

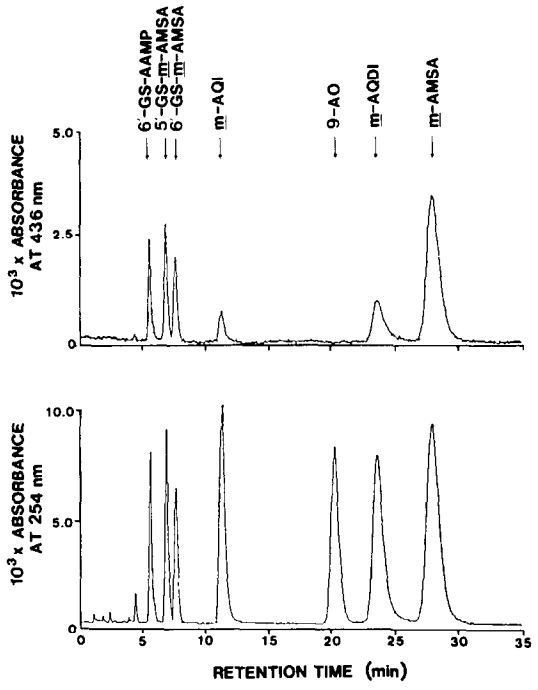

Fig. 3. Representative HPLC profile of the standard spike solution (25 μL) containing *m*-AQDI and potential metabolites. HPLC analysis was performed on a reverse-phase C_{18} Novapak column using a mobile phase of 18% MeCN containing 10 mM TEAP, pH 3.0, at a flow rate of 2.5 mL/min.

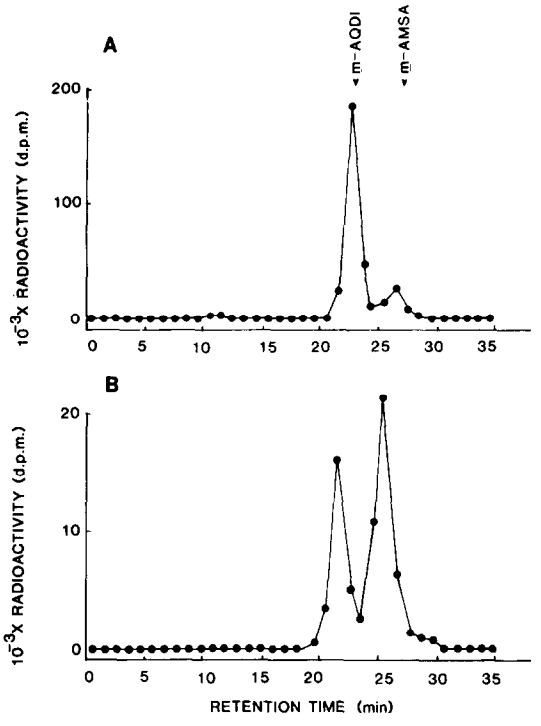

Fig. 4. HPLC profiles demonstrating the instability of [^{3}H]-*m*-AQDI during HPLC. Panel A: 0.4 nmol of [^{3}H]-*m*-AQDI. Panel B: the [^{3}H]-*m*-AQDI peak was collected from a repeat of the above HPLC run, and approximately 0.1 nmol was re-chromatographed.

matographic loadings, indicating the limited reducing capacity of the HPLC system.

The sensitivity of *m*-AQDI to reduction was also evident on incubation at 20 μM [^{3}H]-*m*-AQDI in α-MEM (without serum). Even at 0° only approximately 10% of the *m*-AQDI remained after 5 min, most having been reduced to *m*-AMSA while some was converted to a polar species with a retention time of 6.0 min and peak height ratio of 3.3 (data not shown). This latter species was assumed to be a cysteinyl adduct or mixture of cysteinyl adducts, based on the known reactivity of *m*-AQDI toward thiol compounds and the similarity of retention times and peak height ratios to those of synthetic GSH adducts of *m*-AQDI. Cysteine is the predominant thiol (0.57 mM) in α-MEM.

A variety of sample preparation methods to recover *m*-AQDI and its low MW metabolites from AA8 cells were evaluated (Table 2). While recovery of all species was low using TCA precipitation, good recoveries of most compounds were achieved with 80 or 90% MeCN with higher recoveries of the more lipophilic species (9-AO, *m*-AMSA) at the higher MeCN concentration. However neither *m*-AQI nor

Table 2. Recovery of *m*-AMSA and its potential metabolites from AA8 cells

Metabolite	Amount added (nmol)	% Recovery* Cell lysate TCA	Cell lysate 80% MeCN	Cell lysate 90% MeCN	Supernatant 90% MeCN
6'-GS-AAMP	0.24	18 ± 3	78 ± 6	39 ± 6	91 ± 7
5'-GS-*m*-AMSA	0.22	38 ± 6	98 ± 4	80 ± 8	86 ± 5
6'-GS-*m*-AMSA	0.27	19 ± 3	73 ± 8	52 ± 6	88 ± 10
m-AQI	0.12	<2.5	<2.5	<2.5	73 ± 7
9-AO	0.29	<1.0	55 ± 6	87 ± 7	85 ± 8
m-AQDI	0.53	<1.5	<1.5	<1.5	<3.0
m-AMSA	0.77	5 ± 2	62 ± 2	97 ± 4	92 ± 8

* Recoveries were determined by comparing peak areas (absorbance at 254 nm) for direct HPLC of spike solution (25 μL) with those obtained after adding spike solution (25 μL) to cell lysates or to the supernatant obtained after precipitation of lysates with 90% MeCN. Errors are standard errors of the mean for three to six independent measurements.

m-AQDI was recovered under any of these conditions despite relatively high chromatographic loadings (Table 2). To investigate whether this was due to rapid reaction with macromolecules, spike solution was added to the supernatant obtained after precipitating cellular macromolecules with 90% MeCN. *m*-AQI was now recovered with much higher efficiency but *m*-AQDI was still undetectable (Table 2).

To investigate further the lack of recovery of [^{3}H]-*m*-AQDI, samples (1 nmol) were added to cell preparations at various stages during sample workup (Table 3). When added to lysed cells immediately before addition of MeCN (sample A), 29% of the radioactivity precipitated with the macromolecular fraction, but when added immediately after MeCN only 1.5% was precipitated (sample B) indicating rapid reaction with macromolecules as one fate of *m*-AQDI. *m*-AQDI was not detected by HPLC of the MeCN-soluble fractions, even when the label was added to the deproteinized MeCN-soluble cell extract immediately before chromatography (sample D). All four samples provided very similar chromatograms as illustrated for sample A in Fig. 5 (trace A). In each case three main products were identified on the basis of retention time and peak height ratio: *m*-AMSA constituted approximately 45% of the recovered radioactivity while approximately 40% eluted as the polar GSH adducts 5′- and 6′-GS-*m*-AMSA. A minor radioactive peak at 23 min was identified as AAMP, rather then *m*-AQDI, on the basis of peak height ratio (*ca.* 3). A further minor radioactive peak was observed at a retention time of approximately 10 min, consistent with *m*-AQI, but this could not be identified by peak height ratio because of interference from phenol red carried over from α-MEM (retention time 9.5 min, peak height ratio 0.39). The absence of *m*-AQDI could not be accounted for by reduction during chromatography since HPLC of a similar quantity of total radioactivity from the [^{3}H]-*m*-AQDI stock solution in the same experiment provided 78% recovery as *m*-AQDI (Sample E, Table 3).

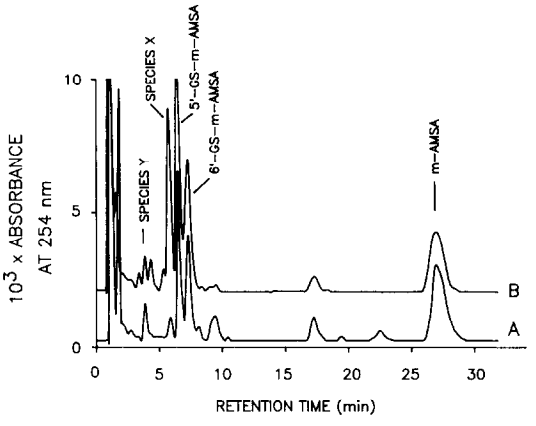

Fig. 5. HPLC of MeCN-soluble extracts prepared 0.5 min after addition of 1 nmol *m*-AQDI to AA8 cell lysates at 0° (trace A) or 0.5 min after addition to intact AA8 cells at 10^7 cells/mL in PBS at 37° (trace B). Ten nanomoles was added to 1 mL of culture from which the cell fraction was recovered by rapid centrifugation. Both chromatograms are extracts from 10^7 cells.

Metabolism of [^{3}H]-m-*AQDI by AA8 cells*

Due to the rapid chemical transformation of *m*-AQDI in α-MEM, the metabolism of [^{3}H]-*m*-AQDI in AA8 cells was studied with cells suspended in PBS. Measurements of total cell-associated radioactivity 0.5 min after addition to suspensions at 37° demonstrated very rapid accumulation of [^{3}H]-*m*-AQDI and/or radioactive metabolites by AA8 cells. Using an intracellular water volume of 800 fL/cell [19] the intracellular concentration of *m*-AQDI equivalents was calculated to be 185 times greater than in the extracellular solution at this time with a slow decline thereafter. The very rapid initial drug uptake was

Table 3. Radioactivity recovered after adding [^{3}H]-*m*-AQDI (1 nmol) to 10^7 AA8 cells at varying stages during preparation for HPLC analysis

	% Total radioactivity					
		MeCN-soluble†				
Sample*	MeCN-insoluble	Polar‡	*m*-AQI	*m*-AQDI	AAMP	*m*-AMSA
A	29.4	28.2	3.2	ND	3.0	31.8
B	1.5	66.3	3.3	ND	2.5	20.5
C	—	66.5	3.3	ND	2.4	20.3
D	—	53.8	2.9	ND	2.8	32.0
E	—	0.4	3.4	78	ND	17.0

* A: Spike added to lysed cells prior to addition of MeCN. B: Spike added to lysed cells immediately after addition of MeCN. C: Spike added to the MeCN extract immediately before freezing. D: Spike added to the MeCN extract after evaporation of MeCN and immediately before redissolving in mobile phase for HPLC. E: Spike added to the mobile phase (free of any cell extract) immediately before HPLC.

† Recoveries of radioactivity from the HPLC column were typically about 85% of the amount injected.

‡ All species with retention times in the range 5 to 9 min.

ND, not detected.

accompanied by formation of covalently bound macromolecular species with MeCN-insoluble radioactivity representing 25 ± 2% of the cell-associated radioactivity 0.5 min after drug addition.

HPLC of MeCN-soluble fractions from cell pellets demonstrated very rapid conversion of [^{3}H]-*m*-AQDI to polar biotransformation products as well as reduction to *m*-AMSA. After 0.5 min the absorbance profile was similar to that observed after spiking deproteinized cell lysates with *m*-AQDI, the major products being *m*-AMSA (retention time 27 min, peak height ratio 2.6), 5'-GS-*m*-AMSA (6.7 min, ratio 3.4) and 6'-GS-*m*-AMSA (7.4 min, ratio 3.2) (Fig. 5, trace B). The profiles were not, however, identical to those obtained with deproteinized lysates. There was, in particular, an increased yield of a polar species (X) with a retention time (6.0 min) and peak height ratio (3.3) similar to the putative cysteinyl adduct observed after incubating *m*-AQDI with α-MEM alone. The retention time of species X was consistently about 0.5 min greater than 6'-GS-AAMP. Quantitation of products by radiochromatography at 0.5 min (Fig. 6A) indicated approximately 26% of the Me-CN-soluble radioactivity (11% of total) eluted as *m*-AMSA. Approximately 66% of the MeCN-soluble radioactivity eluted as the three major polar species, each in approximately equal amounts. Cellular concentrations of species X remained constant for at least 60-min, while concentrations of 5'- and 6'-GS-*m*-AMSA declined rap-

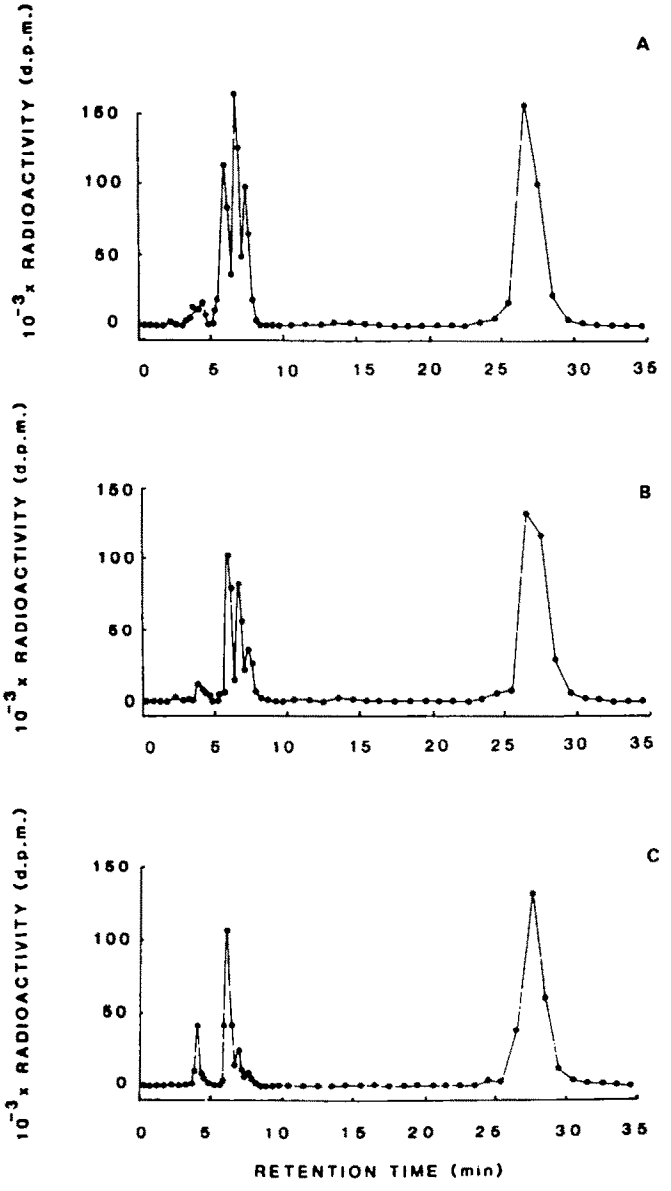

Fig. 6. HPLC of MeCN-soluble radioactive species derived from AA8 cells at various times during incubation with [^{3}H]-*m*-AQDI (10 μM) in PBS at 37°. Incubation times were 0.5 (A), 5 (B) and 60 min (C).

idly and an unidentified polar metabolite (Y) with a retention time of 4.0 min and a peak height ratio of 3.2 gradually increased (Fig. 6).

DISCUSSION

Characterization of the GSH adducts of m-*AQI and* m-*AQDI*

A scheme showing the species formed by reaction of *m*-AQDI and *m*-AQI with GSH is shown in Fig. 7. The structure of the GSH adduct of *m*-AQI has not previously been reported. This study demonstrated that only one regioisomer, the 6′-addition product (6′-GS-AAMP) was formed. Addition of GSH to the 6′-position of the anilino ring was unexpected; previously it had been assumed that nucleophilic addition would be to the 5′ position [7] by analogy with the reported structure of the major species formed by reaction of GSH with *m*-AQDI [12]. However, addition to the 6′- position is consistent with the observation that GSH reacts with the reactive metabolite of paracetamol, *N*-acetyl-*p*-benzoquinone monoimine, by 1,4-addition to the imine rather than the oxygen atom conjugated to the phenyl ring [21]. Reaction of *m*-AQI with the simple sulphur nucleophile methanethiol also results in formation of the 6′-regioisomer [16].

The finding that *m*-AQDI reacts with GSH to form two different species in approximately equal amounts was also unexpected. Previous studies have reported a single product, identified as 5′-GS-*m*-AMSA [12, 15]. In addition to the 5′- addition product, Shoemaker *et al.* [12] observed some minor species by TLC. However, we found by HPLC that the products formed by reacting *m*-AQDI with GSH were very unstable under the TLC conditions described by Shoemaker *et al.* [12], degrading to 9-AA and several other species during chromatography (data not shown). Since the 6′-thioethers of 9-anilinoacridines are more unstable than the corresponding 5′-thiol regioisomers to decomposition during silica chromatography [16], there may have been selective loss of the 6′-GS-*m*-AMSA species by decomposition in the earlier study. In contrast, Gaudich and Przybylski [15] reported that their reaction product was homogeneous by both TLC and HPLC. However, the UV maxima reported for this product were at 248, 263 and 425 nm. These maxima appear to be a composite of the peaks observed for 5′-GS-*m*-AMSA and 6′-GS-*m*-AMSA in the present study, suggesting that the chromatography employed by Gaudich and Przybylski [15] may not have resolved the two regioisomers.

Recovery of potential m-*AMSA metabolites from AA8 cells*

A single-step macromolecule precipitation method was investigated in preference to solvent extraction techniques to seek efficient simultaneous extraction of compounds with widely different physical prop-

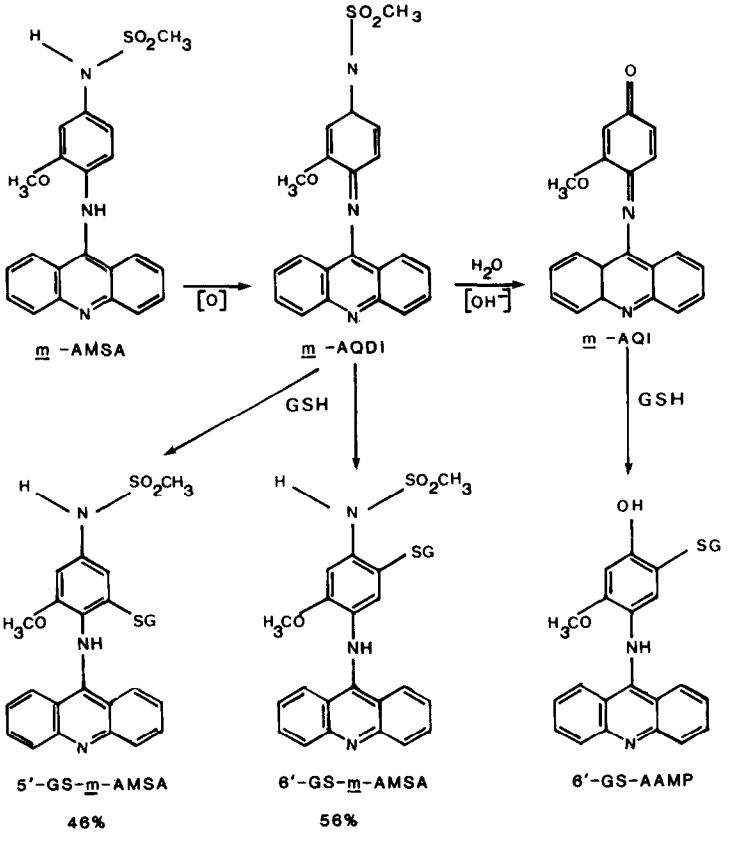

Fig. 7. Structures of *m*-AMSA, *m*-AQDI, *m*-AQI and the species formed by their reaction with GSH.

erties (e.g. the lipophilic weak base *m*-AMSA versus its hydrophilic zwitterionic glutathione derivatives). Precipitation with 90% MeCN provided acceptable recoveries of most species. Recovery of *m*-AMSA by such methods is limited by high affinity non-covalent binding to macromolecules [22, 23] and can be improved by repeated washing of the pellet [19]. The lack of recovery of *m*-AQDI and *m*-AQI reflects their high chemical reactivity rather than non-covalent binding, with rapid formation of protein adducts, reduction products (*m*-AMSA and AAMP, respectively) and thiol adducts in cell lysates. Both 5′ and 6′-GS-*m*-AMSA were identified, on the basis of retention time and peak height ratio, as *m*-AQDI products. These were observed in approximately equal amounts and were major products, representing >50% of total radioactivity even when *m*-AQDI was added to deproteinized cell extracts immediately before chromatography, indicating rapid formation by a non-enzymatic mechanism.

Pathways for biotransformation of m-*AQDI in AA8 cells*

In view of the high chemical reactivity of *m*-AQDI in cell lysates at 0° the rapid biotransformation in cells at 37° was expected. Analysis of the radioactive species formed in AA8 cells after incubation with [^{3}H]-*m*-AQDI indicates conversion in these cells, in less than 1 min, to *m*-AMSA, polar biotransformation products and covalently-bound macromolecular adducts, each in approximately equal yield.

Reduction of *m*-AQDI to *m*-AMSA is clearly a very facile process, as might be anticipated from the 2-electron reduction potential for the *m*-AQDI/*m*-AMSA couple at pH 7.4 (415 mV versus n.h.e. [24]). Studies with [^{3}H]-*m*-AQDI indicate that some reduction of *m*-AQDI occurs during HPLC. Since a smaller proportion of *m*-AQDI is reduced when larger amounts of drug are chromatographed, reduction may occur at only a limited number of sites during transit through the HPLC apparatus. Not all of the *m*-AMSA detected in samples from cells treated with [^{3}H]-*m*-AQDI can be due to reduction during chromatography since high levels of *m*-AMSA were observed in the absence of detectable *m*-AQDI, yet when similar amounts of *m*-AQDI (0.9–6 nmol) were loaded directly onto the HPLC column only 17–32% of the *m*-AQDI was converted to *m*-AMSA. These observations indicate that some intracellular reduction of *m*-AQDI to *m*-AMSA must occur. While reduction in α-MEM is presumably due to ascorbic acid, the intracellular conversion of *m*-AQDI to *m*-AMSA is probably mediated by reduced pyridine nucleotides [25].

In like manner, the small quantities of AAMP observed in extracts from cell preparations treated with [^{3}H]-*m*-AQDI must arise from biological reduction of *m*-AQI, rather than the reduction of *m*-AQI during HPLC, since when approximately 2×10^4 dpm *m*-AQI was observed by HPLC of [^{3}H]-*m*-AQDI-treated cell extracts, equivalent radioactivity was recovered as AAMP (Table 3, samples A–D). Yet AAMP was not observed on chromatography of a [^{3}H]-*m*-AQDI solution containing 6.8×10^4 dpm *m*-AQI (Table 3, sample E).

Any reduction of *m*-AQDI to *m*-AMSA in cells or during analysis is a potential difficulty in attempting to detect oxidative metabolites of *m*-AMSA. However, the observation of rapid formation of polar biotransformation products is of greater significance to the present study. The major polar biotransformation products arise from reactions with GSH, the 5′- and 6′- addition products being identified from a comparison of chromatographic and absorbance properties with those of the authentic compounds. The same products are formed rapidly in ice-cold cell lysates or deproteinized MeCN extracts indicating that enzymic catalysis is not required for formation of 5′- and 6′-GA-AMSA. These comparisons do not exclude the possibility of significant rate enhancement by GSH transferases as has recently been suggested by Robertson *et al.* [26]. In fact there are differences between the polar biotransformation products formed in intact cells at 37° or lysates at 0°, particularly in the increased yield of species X in intact cells (Fig. 5), suggesting that the spectrum of products may be modified by enzyme systems in intact cells. Species X and Y have not been identified, but might respectively represent an adduct formed with another nucleophile such as cysteine, or the 9-thioether formed by thiolysis of 5′- or 6′-GS-*m*-AMSA in the presence of high concentrations of GSH [15].

Implications for oxidative activation of m-*AMSA as a mechanism of cytotoxicity*

An investigation of the metabolic fate of [^{3}H]-*m*-AMSA in cultured AA8 cells has been reported recently [19]. After a 1 hr exposure to [^{3}H]-*m*-AMSA at 37°, 98–99% of the cell-associated radioactivity was recovered in the supernatant after precipitation and extensive washing of macromolecules with MeCN. A small amount of radioactivity (approximately 1% of the total) remained associated with the pellet, reflecting the formation of covalently-bound macromolecular adducts. HPLC analyses of the MeCN-soluble fractions showed that ≥96% of the radioactivity detected in the first MeCN wash fraction was unchanged *m*-AMSA, with unchanged *m*-AMSA also accounting for >90% of the radioactivity in subsequent wash fractions. No *m*-AQDI was detected in the MeCN extracts.

The present study indicates that failure to detect *m*-AQDI by HPLC does not of itself preclude significant oxidative metabolism of *m*-AMSA in AA8 cells, since the primary oxidation product, *m*-AQDI, is highly unstable. But the data described here indicate that if *m*-AMSA were being oxidized to *m*-AQDI, approximately 30% of the *m*-AQDI generated would be trapped as low molecular weight thiol conjugates. After incubating cells with [^{3}H]-*m*-AMSA for 1 hr at 37°, <0.4% of the total cell-associated radioactivity eluted with chromatographic properties characteristic of the thiol adducts [19], implying that the rate of oxidation of *m*-AMSA to *m*-AQDI by AA8 cells is less than 1% per hr. This upper limit depends upon the assumption that the yields of thiol adducts formed from low steady state levels of *m*-AQDI generated intracellularly from *m*-AMSA would be similar to those observed in the

present studies after exposing cells to high concentrations of *m*-AQDI.

Given this proviso, the present study indicates a lack of oxidative metabolism of *m*-AMSA to *m*-AQDI by AA8 cells and therefore suggests that cytotoxicity of *m*-AMSA in this cell line is due to the unmodified parent drug. The demonstration that cytotoxicity of *m*-AMSA in Chinese hamster cell lines is independent of oxygen tension [20, 27] also argues against the involvement of *m*-AQDI since its formation via cytochrome P450-dependent oxidation requires oxygen as a co-substrate [7]. The lack of cytochrome P450 in cultured cell lines [28] and tumours [29] would render such a mechanism unlikely, but the present study suggests there are no (other) enzymatic or non-enzymatic oxidative systems capable of forming *m*-AQDI at appreciable rates in these *m*-AMSA-sensitive tumour cells. Further evidence that *m*-AMSA cytotoxicity is not due to formation of *m*-AQDI is provided by the finding that *m*-AQDI depletes intracellular GSH but that m-AMSA does not at equivalent cytotoxicity.* In addition, Jurlina *et al.* [30] reported that the cytotoxic potency of a series of anilino-ring substituted *m*-AMSA analogues is independent of sensitivity to oxidation.

The lack of requirement for oxidative metabolism in the cytotoxicity of *m*-AMSA in cultured tumour cells suggests the parent drug is probably responsible for antitumour activity *in vivo*, at least in tumours with a low capacity for oxidative xenobiotic metabolism. It does not, of course, preclude a significant role for such metabolic activation in toxicity towards cytochrome P450-rich normal tissues such as liver, and allows the possibility that modulation of oxidative metabolism could be used to alter the pharmacokinetics and hepatotoxicity of anilinoacridine antitumour drugs.

REFERENCES

1. Louie AC and Issell BF, Amsacrine (AMSA)—a clinical review. *J Clin Oncol* **3**: 562–592, 1985.
2. Nelson EM, Tewey KM and Liu LF, Mechanism of antitumor drug action: poisoning of mammalian DNA topoisomerase II on DNA by 4′-(9-acridinylamino)-methanesulfon-*m*-anisidide. *Proc Natl Acad Sci USA* **81**: 1361–1365, 1984.
3. Tewey KM, Chen GL, Nelson EM and Liu LF, Intercalative antitumor drugs interfere with the breakage-reunion reaction in mammalian DNA topoisomerase II. *J Biol Chem* **259**: 9182–9187, 1984.
4. Glisson BS and Ross WE, DNA topoisomerase II: a primer on the enzyme and its unique role as a multidrug target in cancer chemotherapy. *Pharmacol Ther* **32**: 89–106, 1987.
5. Wilson WR, Harris NM and Ferguson LR, Comparison of the mutagenic and clastogenic activity of amsacrine and other DNA-intercalating drugs in cultured V79 Chinese hamster cells. *Cancer Res* **44**: 4420–4431, 1984.
6. Ferguson LR and Baguley BC, Relationship between induction of chromosome damage and cytotoxicity for amsacrine and congeners. *Cancer Treat Rep* **68**: 625–630, 1984.
7. Shoemaker DD, Cysyk RL, Gormley PE, DeSouza JJV and Malspeis L, Metabolism of 4′-(9-acridinylamino)methanesulfon-*m*-anisidide by rat liver microsomes. *Cancer Res* **44**: 1939–1945, 1984.
8. Wong A, Cheng H-Y and Crooke ST, Identification of the active species in deoxyribonucleic acid breakage induced by 4′-(9-acridinylamino)methanseulfon-*m*-anisidide and copper. *Biochem Pharmacol* **35**: 1071–1078, 1986.
9. Wong A, Huang C-H, Hwang S-M, Prestayko AW and Crooke ST, Formation of the thiol adducts of 4′-(9-acridinylamino)-methanesulfon-*m*-anisidide and their binding to deoxyribonucleic acid. *Biochem Pharmacol* **35**: 1655–1662, 1986.
10. Wilson WR, Cain BF and Baguley BC, Thiolytic cleavage of the anti-tumour compound 4′-(9-acridinylamino)-methanesulphon-*m*-anisidine (*m*-AMSA, NSC156303) in blood. *Chem Biol Interact* **18**: 163–178, 1977.
11. Cysyk RL, Shoemaker D and Adamson RH, The pharmacologic disposition of 4′-(9-acridinyl-amino)-methanesulfon-*m*-anisidide in mice and rats. *Drug Metab Dispos* **5**: 579–590, 1977.
12. Shoemaker DD, Cysyk RL, Padmanabhan S, Bhat HB and Malspeis L, Identification of the principal biliary metabolite of 4′-(9-acridinylamino)methanesulfon-*m*-ansidide in rats. *Drug Metab Dispos* **10**: 35–39, 1982.
13. Cain BF, Wilson WR and Baguley BC, Structure–activity relationships for thiolytic cleavage rates of antitumor drugs in the 4′-(9-acridinylamino)methanesulfonanilide series. *Mol Pharmacol* **12**: 1027–1035, 1976.
14. Przybylski M, Cysyk RL, Shoemaker D and Adamson RH, Identification of conjugation and cleavage products in the thiolytic metabolism of the anticancer drug 4′-(9-acridinyl-amino)methanesulfon-*m*-anisidide. *Biomed Mass Spectrom* **8**: 485–491, 1981.
15. Gaudich K and Przybylski M, Field desorption mass spectrometric characterization of thiol conjugates related to the oxidative metabolism of the anticancer drug 4′-(9-acridinylamino)-methanesulfon-*m*-anisidide. *Biomed Mass Spectrom* **10**: 292–299, 1983.
16. Lee HH, Palmer BD and Denny WA, Reactivity to nucleophiles of quinoneimine and quinonediimine metabolites of the antitumor drug amsacrine and related compounds. *J Org Chem* **53**: 6042–6047, 1988.
17. Black M, Acetaminophen hepatotoxicity. *Annu Rev Med* **35**: 577–593, 1984.
18. Maftouh M, Meunier G, Dugue B, Monsarrat B, Meunier B and Paoletti C, Metabolism of the anti-tumour drugs N^2-methyl-9-hydroxyellipticinium acetate (NSC 264137) and N^2-methyl-9-hydroxyolivacinium acetate in the rat: preliminary identification of biliary 9-(*O*)-glucuronide and 10(*S*)-glutathione conjugates. *Xenobiotica* **13**: 303–310, 1983.
19. Robbie MA, Baguley BC, Denny WA, Gavin JB, Wilson WR, Mechanism of resistance of noncycling mammalian cells to 4′-(9-acridinylamino)-methanesulfon-*m*-anisidide: comparison of uptake, metabolism, and DNA breakage in log- and plateau-phase Chinese hamster fibroblast cell cultures. *Cancer Res* **48**: 310–319, 1988.
20. Wilson WR, Denny WA, Twigden SJ, Baguley BC and Probert JC, Selective toxicity of nitracrine to hypoxic mammalian cells. *Br J Cancer* **49**: 215–223, 1984.
21. Johnston D, Smith DI and Andrews RS, Some observations on the synthesis of the mercapturic acid conjugate of paracetamol. *J Chem Res (S)*: 386–387, 1986.
22. Wilson WR, Baguley BC, Wakelin LPG and Waring MJ, Interaction of the antitumor drug 4′-(9-acridinylamino)methane- sulfon-*m*-anisidide and related acridines with nucleic acids. *Mol Pharmacol* **20**: 404–414, 1981.

* W. R. Wilson, M. A. Robbie, S. M. Pullen and G. J. Finlay, manuscript in preparation.

23. Paxton JW, Jurlina JL and Foote SE, The binding of amsacrine to human plasma proteins. *J Pharm Pharmacol* **38**: 432–438, 1986.
24. Anderson RF, Packer JE and Denny WA, One-electron redox chemistry of amsacrine, mAMSA [9-(2-methoxy - 4 - methylsulphonyl- aminoanilino)acridinium], its quinone diimine, and an analogue. A radiolytic study. *J Chem Soc Perkin* **II**: 489–496, 1988.
25. Wong A, Huang C-H and Crooke ST, Mechanism of deoxyribonucleic acid breakage induced by 4′-9-acridinylamino)methanesulfon-*m*-anisidide and copper: role for cuprous ion and oxygen free radicals. *Biochemistry* **23**: 2946–2952, 1984.
26. Robertson ICG, Kestell P, Dormer RA and Paxton JW, Involvement of glutathione in the metabolism of the anilinoacridine antitumour agents CI-921 and amsacrine. *Drug Metab Drug Interact*, in press.
27. Wilson WR, Giesbrecht JL, Hill RP and Whitmore GF, Toxicity of 4′-(9-acridinylamino)methanesulfon-*m*-anisidide in experimental and plateau-phase Chinese hamster cell cultures. *Cancer Res* **41**: 2809–2816, 1981.
28. Wiebel FJ, Lambiotte M, Singh J, Summer K-H and Wolff T, Expression of carcinogen-metabolizing enzymes in continuous cultures of mammalian cells. In: *Biochemical Basis of Chemical Carcinogenesis* (Eds. Greim H, Jung R, Kraemer M, Marquardt H, Oesch F), pp. 77–78. Raven Press, New York, 1984.
29. El Mouelhi M, Didolkar MS, Elias EG, Guengerich EP and Kauffman FC, Hepatic drug-metabolizing enzymes in primary and secondary tumors of human liver. *Cancer Res* **47**: 460–466, 1987.
30. Jurlina JL, Linsay A, Packer JE, Baguley BC and Denny WA, Redox chemistry of the 9-anilinoacridine class of antitumour agents. *J Med Chem* **30**: 473–480, 1987.